

Photocatalytic degradation of aqueous phenanthrene in a slurry photocatalytic reactor: optimization and modelling

C. Nirmala Rani* and S. Karthikeyan

Centre for Environmental Studies, Anna University, Chennai 600 025, India

A photoreactor with 254 nm, 16 W UV lamp was evaluated for phenanthrene (PHE) degradation. The effect of operating variables such as initial PHE concentration (1000–1500 µg/l), catalyst dosage (0.1–0.9 g/l) and pH (3.0–9.0) on PHE degradation was investigated in detail. The batch study of photocatalytic process showed 83.5% PHE degradation and 60.2% TOC removal for optimized values (PHE concentration – 1000 µg/l, TiO₂ dosage – 0.5 g/l and pH – 3.0) during 3 h reaction. The photocatalytic degradation of PHE was found to follow pseudo-first-order kinetics. The results obtained from continuous process revealed that nano TiO₂ could be used for industrial applications because of its potential for long-term operations. Response surface methodology (RSM) with Design Expert software was used to analyse the obtained experimental data.

Keywords: Degradation, kinetic constants, mineralization, photocatalysis, TiO₂.

POLYCYCLIC aromatic hydrocarbons (PAHs) are persistent organic pollutants (POPs) with carbon and hydrogen atoms and composed of multiple benzene rings. Because of their carcinogenic, mutagenic and toxic effects, they have significant impact on both human and environment^{1,2}. They are generally found in air, soil and water and their sources may be natural or anthropogenic. Natural sources include volcanic eruption and forest fires^{3,4}. Anthropogenic sources may be either petrogenic or pyrogenic. Petrogenic sources contribute to the production of high molecular weight (HMW) PAHs and their sources are oil spills from crude petroleum^{4–6}. Meanwhile, low molecular weight (LMW) PAHs are generated by pyrogenic sources that include partial combustion of coal, petroleum and wood burning^{4,7}. PAHs contaminated natural waters and the usage of pipes coated with coal tar in water supply systems cause their presence in drinking water⁸. Adsorption by means of activated carbon or other adsorbents, thermal oxidation, ozonation and chlorination, etc. could eliminate water bound PAHs⁹. However, these conventional treatment methods are inefficient for

abating PAHs from water. Therefore, cost, energy efficient and eco-friendly methods are needed to eliminate them completely from water.

Advanced oxidation processes (AOPs) were found to be very effective in removing toxic, non-biodegradable, recalcitrant organic micropollutants from water¹⁰ through the generation of hydroxyl radical OH• which is highly reactive and has a high oxidation potential of 2.8 V. Ultraviolet (UV) radiation proved to be much more efficient in degrading a wide spectrum of organic micro pollutants with oxidants (hydrogen peroxide (H₂O₂) or titanium dioxide (TiO₂))^{11,12}. Among AOPs, heterogeneous photocatalysis was found successful for removal of organic pollutants¹³ with the photocatalyst TiO₂ (ref. 14). These methods produce significant changes in the chemical structure of compounds and could be used alone or in combination with conventional methods¹⁵. Meanwhile, P25 Degussa TiO₂, which is a mixture of 70% anatase and 30% rutile has been widely used by researchers as a photocatalyst for degradation of PAHs in aqueous solutions^{16,17} and soil surfaces¹⁸. During semi-conductor photocatalysis, electron-hole pairs are formed which leads to a stepwise oxidation of organic molecules^{19,20}.

Phenanthrene (PHE) is one among 16 PAHs classified by US EPA as priority pollutants¹⁹. Though numerous studies were carried out on various PAHs as individual and total model compound^{21–23}, limited studies are available on the photocatalytic degradation of aqueous phenanthrene^{24,25} using real wastewater. Lin and Valsaraj²¹ developed a photocatalytic reactor in which 4 UV lamps of 1–8 mW/cm² intensity were placed around the reactor. Vela *et al.*²² studied the photocatalytic degradation of PHE using natural sunlight utilizing ZnO and TiO₂ as photocatalysts. Previous studies revealed that the position of UV lamp and the intensity of the lamp play significant role during photocatalytic degradation. Therefore the aim of this study was to investigate the degradation of PHE during photocatalysis in a batch and continuous photocatalytic reactor employing Degussa P25 TiO₂ as catalyst. In this photoreactor, a 16 W UV lamp of 254 nm was centrally placed to give uniform irradiation. The effect of various operating variables including PHE concentration, TiO₂ dosage and pH on PHE degradation were discussed. The photocatalytic degradation kinetics of aqueous PHE

*For correspondence. (e-mail: nirmalacrani@gmail.com)

and the corresponding TOC removal were also studied. Response surface methodology with central composite design was used to examine the individual effects of variables (PHE concentration, catalyst dosage and pH) and their interactive effects on PHE and TOC removal efficiencies.

Materials and methods

Materials

Phenanthrene ($C_{14}H_{10}$, MW-178) and titanium oxide (Evonik Degussa P25, Germany TiO_2 , 21 nm TEM size) were purchased from Sigma Aldrich. The photocatalyst TiO_2 was a mixture of 70% anatase and 30% rutile with BET surface area of $50\text{ m}^2/\text{g}$ and band gap 3.2 eV. Hydrochloric acid (36.5–38.0%), sodium hydroxide (99%), dichloromethane, acetonitrile and hexane purchased from Merck were of HPLC grade. TOC analysis was carried out with double distilled water (Merck).

Experimental setup

Figure 1 shows the schematic of a laboratory scale slurry photoreactor. The reactor of 2.1 litre volume made up of plexiglas material consisted of a 16 W, 254 nm low

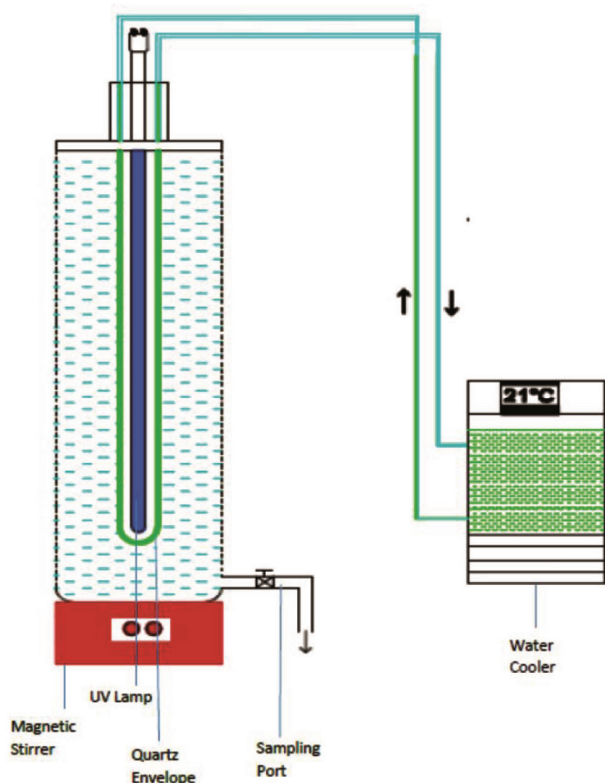


Figure 1. Schematic diagram of a laboratory scale photocatalytic reactor.

pressure Hg UV-C lamp. In order to provide uniform irradiation, UV-C lamp was placed at the centre of the reactor. In order to prevent the thermal catalytic effect, the lamp was enclosed by a double-layered quartz glass tube through which water was recirculated. The slurry was continuously stirred using magnetic stirrer.

Analytical methods

Experimental procedure: The reaction mixture was prepared by adding known concentrations of PHE and catalyst in distilled water. During all experiments, the reaction sample was kept in dark (in the absence of UV light) for 30 min so that the PHE molecules would adsorb on the catalyst surface. Batch studies were carried out for 3 h with different initial concentrations (1000–1500 $\mu\text{g}/\text{l}$) of PHE and catalyst dosage 0.5 g/l. After optimizing the pollutant concentration, the pH of the reaction mixture was varied from 3 to 9 and optimized. The required pH variations were carried out by 0.1 M NaOH and 0.1 M HCl. Samples were collected at 30 min interval and centrifuged for 5 min at a speed of 4000 rpm. The temperature during the reaction was maintained at $21 \pm 1^\circ\text{C}$. To provide reproducibility of the results, each experiment was performed at least twice.

Degradation and mineralization study: PHE was quantified by GC-MS Agilent Technology system consisting of a 6890 GC equipped with a DB-5MS mid polar (5% phenyl 95% polydimethylsiloxane stationary phase) column of $30\text{ m} \times 0.25\text{ mm}$ (inner dia). Mass spectrometer (5973) detection was operated in an electron impact mode with ionization energy of 70 eV. A temperature of 280°C was maintained as injection and interface temperatures of the program and the carrier gas used was helium. The initial temperature of the oven was held at 40°C (1 min hold). The temperature ramps were 40°C (1 min hold) and $130\text{--}280^\circ\text{C}$ (5 min hold). A sample volume of $1\ \mu\text{l}$ was injected at a flow rate of 1 ml/min.

Liquid–liquid extraction (LLE) method was used to concentrate the sample and the PHE was quantified by gas chromatography (GC) mass spectrometry (MS) detection. During liquid–liquid extraction, for 30 ml sample, 90 ml of dichloromethane (DCM) was added in a separating funnel and was shaken well for 10 min after which it was allowed to rest for 10 min. The organic extract was allowed to pass through a funnel containing sodium sulphate anhydride and collected into a glass tube. This extraction procedure was repeated twice and the volume was concentrated to 5 ml in DCM and evaporated. This final extract was concentrated to 2 ml and analysed by GC-MS. In order to evaluate the mineralization efficiency of PHE during photocatalytic treatment, total organic carbon (TOC)²⁶ was measured. All samples and standards were stored in amber bottles to minimize photolytic decomposition.

The mineralization efficiency was determined by analysing the TOC of the samples using TOC-VCPH/CPN PC-controlled TOC Analyser (SHIMADZU Corporation, KYOTO, Japan) equipped with an NDIR detector (680°C combustion catalytic oxidation technique). The LOD of the instrument was 4 µg/l and accuracy <2%. The repeatability of the measurements from GC-MS and TOC analyser was verified by standard deviation (SD) and coefficient of variation (CV). The errors were estimated to be within ±5% during measurement for all samples. Kinetic degradation was studied during batch experiment. Stock solutions of PHE were prepared with double distilled water and 0.5 g/l of TiO₂ photocatalyst was added to the reaction mixture.

Continuous studies: The initial concentration of PHE = 1000 µg/l and TiO₂ = 0.5 g/l were applied for continuous process. The feed solution of 9 litre containing 1000 µg/l PHE and 0.5 g/l TiO₂ with a HRT of 140 min was applied to the reactor continuously. The volume of sample entering the reactor (inflow) and the volume of sample leaving (outflow) were kept equal as 15 ml/min so that the constant volume of the reaction mixture was maintained. The reproducibility of the results was confirmed by repeating each experiment at least twice.

Experimental design data analysis: Response surface methodology (RSM) based on central composite design (CCD) was applied to optimize the photocatalytic degradation of PHE and TOC removal. The three parameters, PHE concentration, TiO₂ dosage and pH were assessed for two responses; PHE degradation and TOC removal. The obtained experimental data was analysed by Design-Expert software.

Results and discussion

Evaluation of PHE-TiO₂ dark adsorption

Dark control tests were conducted to evaluate the possible adsorption of PHE on TiO₂ photocatalyst surface. For dark adsorption, 2.1 litre sample containing 1000 µg/l PHE, 0.5 g/l TiO₂ was covered with aluminium foil sheet and kept in a dark environment for 24 h. The sample pH of 6.1 was not modified. The sample was analysed for PHE concentration and the results showed that only 8% of PHE molecules were adsorbed onto TiO₂ surface which may be due to the effect of electrostatic repulsion. These tests were carried out to reduce the errors due to non-photocatalytic phenomena (adsorption).

Photocatalytic experiments

Batch experiments: Photocatalytic experiments were performed for varying PHE concentrations (1000, 1100,

1300, 1400 and 1500 µg/l), TiO₂ dosage (0.1, 0.3, 0.5, 0.7 and 0.9 g/l) and pH (3, 6.1, 7 and 9). The pH of the sample was 6.1. Samples were collected at a time interval of 30 min for 3 h, centrifuged, decanted and analysed. During all the experiments, the temperature inside the reactor was maintained at 21 ± 1°C.

Effect of initial PHE concentrations: The effect of PHE concentrations on degradation and TOC removal efficiencies was studied by varying the PHE concentrations from 1000 to 1500 µg/l (Figure 2a). The samples of 15 ml were collected at every 30 min interval and the PHE concentration analysed by GC-MS. During this study, it was noticed that the increase in initial PHE concentration from 1000 to 1500 µg/l decreased both degradation (84% to 31%) and mineralization (60% to 24%) efficiencies. The reason could be: when PHE concentration was increased, in addition to TiO₂, the compound (PHE) molecules (UV light screening effect of PHE) also tend to absorb light photons which in turn minimized the energy available for hydroxyl radical generation. Since the light intensity and irradiation time were constant, increase in PHE concentration reduced hydroxyl radical generation. Similar results were reported earlier for dye removal²⁷⁻³¹. Furthermore, the initial steeper trend in the graph at the early stages indicated the presence of sufficient catalyst surface in the reaction mixture for PHE degradation. However at later stages, the intermediate compounds which were formed during the breakdown of compound molecules competed with the PHE molecules for active sites and lowered the rate of degradation. Similar behaviour was reported earlier on dyes; reactive red 2 (ref. 27), acid red and acid green³².

Effect of TiO₂ loading: The optimum TiO₂ dosage was examined by varying the TiO₂ dosage from 0.1 to 0.9 g/l at sample pH. The results are shown in Figure 2b. As the TiO₂ loading was increased from 0.1 to 0.5 g/l, the PHE degradation efficiency also increased (from 50% to 84%) and further increase in catalyst dosage reduced the degradation efficiency (from 84% to 46%). The reason could be; while increasing the TiO₂ dosage from 0.1 to 0.5 g/l, the amount of catalyst surface also increases, which in turn enhances the adsorption of photons and PHE molecules. However, further increase of TiO₂ loading from 0.5 to 0.9 g/l, caused decrease in degradation efficiency. This was due to the reduction in surface area exposed for irradiation due to light screening caused by the excess amount of photocatalyst. Increase in photocatalyst concentration led to increase in solution opacity due to increase of solution turbidity and hence the penetration ability of photons through the solution decreased consequently^{23,33,34}.

Effect of pH: During this study it was observed that photocatalytic degradation rate of PHE was greater when

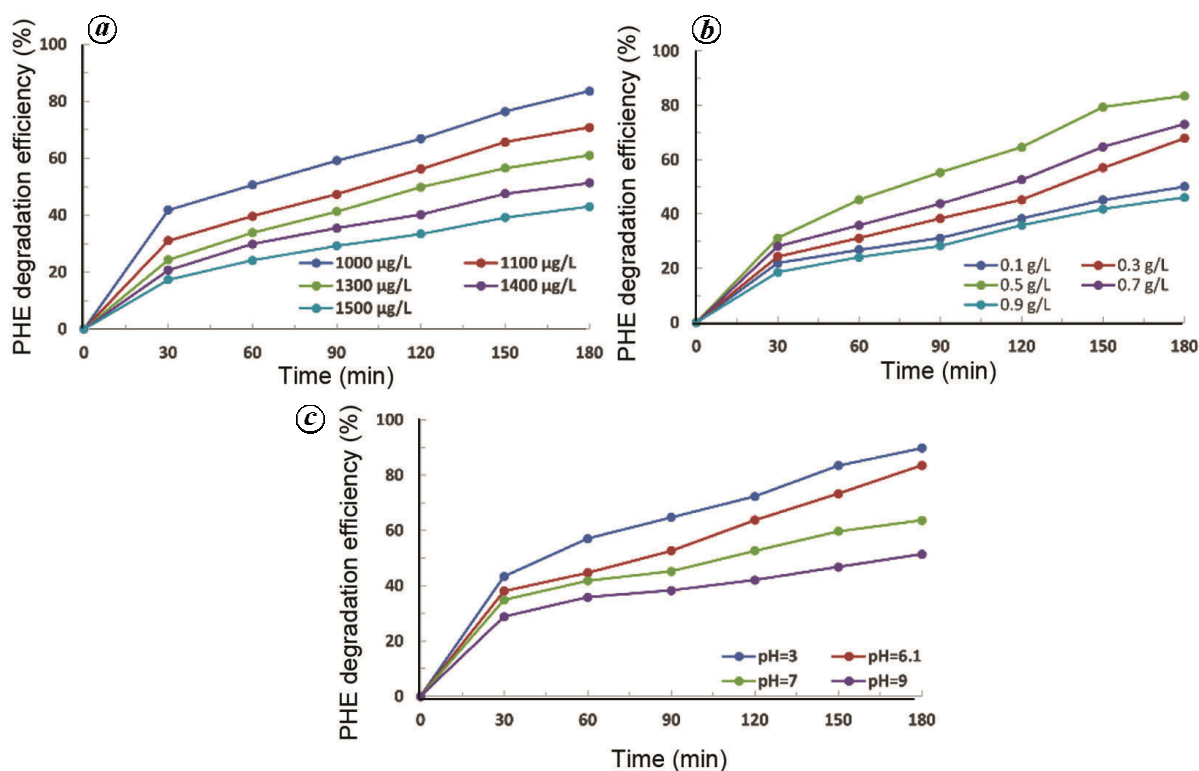


Figure 2. The effect of (a) PHE concentrations, (b) TiO₂ loadings and (c) pH on PHE degradation efficiency.

the reaction mixture was acidic than it was basic. The effect of pH on photocatalytic degradation of PHE has been demonstrated in Figure 2c. It reveals that at pH 3, the maximum degradation efficiency of PHE was 84% while at pH 9, the lowest PHE degradation efficiency of 51% was observed (1000 µg/l PHE and 0.5 g/l TiO₂). This explanation could be with respect to: (i) the surface charge of TiO₂ and (ii) agglomerated sizes of TiO₂.

The isoelectric point (P_{zc}) of TiO₂ (Degussa P25) catalyst is 6.8. At P_{zc} , the absence of electrostatic force minimizes the interaction between TiO₂ particles and PHE molecules. However, when $pH > P_{zc}$, the TiO₂ catalyst surface was negatively charged and repulsed PHE molecules in water thereby reducing the degradation efficiency. On the contrary, when $pH < P_{zc}$, the TiO₂ surface was positively charged and because of the attractive forces, more anionic PHE molecules were adsorbed onto TiO₂ surface which in turn enhanced the degradation and mineralization efficiencies. Another explanation could be with respect to the particle size of TiO₂. When dispersed in water, TiO₂ particles agglomerates and their agglomerated sizes vary from 0.2 to 1.2 µm (ref. 35). The agglomeration of TiO₂ particles also affected the degradation rate. The agglomerated sizes of TiO₂ measured in this study were 220, 331 and 1253 nm and for the pH 3, 6.1 and 9 respectively.

Kinetics of PHE degradation and mineralization: In this study, the obtained experimental PHE degradation data

with respect to initial PHE concentrations followed pseudo-first-order kinetics (eq. (1))

$$\frac{d[\text{PHE}]_t}{dt} = k[\text{PHE}]_0,$$

$$\ln \frac{[\text{PHE}]_0}{[\text{PHE}]_t} = -kt, \quad (1)$$

where (PHE)_t (µg/l) is the PHE concentration at time t ; [PHE]₀ (µg/l) is the initial PHE concentration; t (min) is the reaction time and k (min⁻¹) is the pseudo first order rate constant. Regression analysis was used to determine the first-order rate constants. Table 1 shows the pseudo first-order rate constant (k and R^2 values for various PHE concentrations). The plot for $\ln[\text{PHE}]_0/[\text{PHE}]_t$ and $\ln[\text{TOC}]_0/[\text{TOC}]_t$ versus t are depicted in Figure 3a and b. The calculated correlation coefficient (R^2 values) (shown in Table 1) confirmed the first-order kinetics of PHE degradation. Furthermore, it was observed that the increase in initial PHE concentration from 1000 to 1500 µg/l, decreased the rate constant from 0.0098 to 0.0032 for PHE degradation and 0.018 to 0.006 for TOC removal. Similar results were observed from other studies^{34,36-39}.

Continuous flow experiments: The optimized operating parameters during batch mode were [PHE] = 1000 µg/l, [TiO₂] = 0.5 g/l and pH = 3. The continuous mode was

Table 1. Pseudo first order kinetic data for PHE degradation and TOC removal

PHE concentration (µg/l)	PHE degradation		TOC removal	
	<i>K</i> (min ⁻¹)	<i>R</i> ² value	<i>K</i> (min ⁻¹)	<i>R</i> ² value
1000	0.0098	0.994	0.018	0.9964
1100	0.0066	0.9972	0.0127	0.9926
1300	0.0053	0.9948	0.0093	0.9835
1400	0.004	0.9919	0.0077	0.9676
1500	0.0032	0.9904	0.006	0.9955

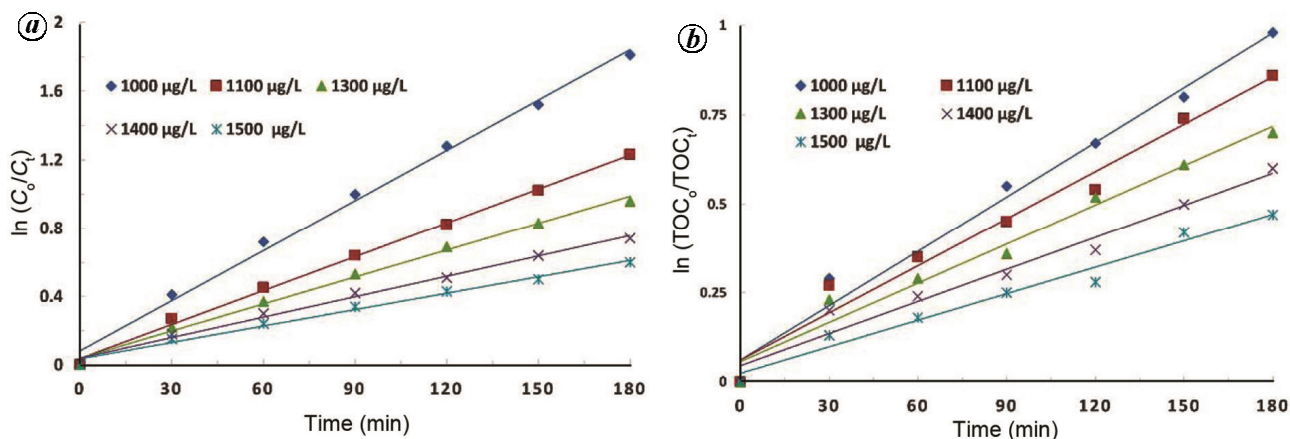


Figure 3. The pseudo first order kinetic plot for (a) PHE degradation and (b) TOC removal efficiency ([PHE] = 1000 µg/l, [TiO₂] = 0.5 g/l).

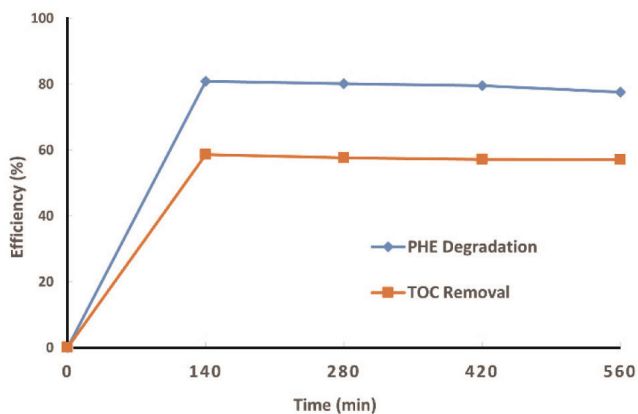


Figure 4. PHE degradation and TOC removal in the photocatalytic reactor during continuous process ([PHE] = 1000 µg/l, [TiO₂] = 0.5 g/l).

operated with optimized parameters. Figure 4 is the graphical illustration of the evaluation of slurry photocatalytic reactor for PHE degradation and TOC removal. The maximum PHE degradation and TOC removal obtained during experimentation were 81% and 58% respectively. The slight decrease in removal efficiency observed was due to the deposition of catalyst particles on the surface of the reactor wall which in turn reduced the availability of TiO₂ particles for photodegradation. By

increasing the reaction time, degradation efficiency could be enhanced⁴⁰.

Optimization of PHE photocatalytic degradation and RSM modelling

Based on the experimental data and CCD matrix, two second order polynomial expressions were obtained and are shown in eqs (2) and (3).

$$\begin{aligned} \% \text{ Removal efficiency } (Y_1) = & -6303.73082 + 3.97076 * x_1 \\ & - 5613.92697 * x_2 + 998.28833 * x_3 - 0.62136 * x_1 x_2 \\ & - 0.60305 * x_1 x_3 - 785.45933 * x_2 x_3 \\ & - 2.24061E-005 * x_1^2 - 202.96930 * x_2^2 - 0.70157x_3^2, \end{aligned} \quad (2)$$

$$\begin{aligned} \% \text{ TOC Removal } (Y_2) = & 285.50480 + 0.040837 * x_1 \\ & - 368.01025 * x_2 - 49.40857 * x_3 + 0.13552 * x_1 x_2 \\ & + 0.032403 * x_1 x_3 + 37.85805 * x_2 x_3 - 1.37461E \\ & - 0.0004 * x_1^2 - 21.4711 * x_2^2 - 0.44089 * x_3^2. \end{aligned} \quad (3)$$

The positive signs in the model indicate the synergetic effects while the negative signs indicate antagonistic effects. The parameters used in the CCD and the experimental data in the CCD for the study of photocatalytic degradation of PHE are shown in Tables 2 and 3.

ANOVA (analysis of variance) was used to test the significance and adequacy of the model. The results of

Table 2. Parameters used in central composite design

Parameter	Symbol	Low (-1)	Centre (0)	High (+1)
x_1	PHE conc (micrograms per litre)	1000	1250	1500
x_2	Catalyst dosage (g/l)	0.1	0.5	0.9
x_3	pH	3	6	9

Table 3. Experimental data in the central composite design for the study of photocatalytic degradation of PHE

Std	Run	Block	Factor 1			Response 1 PHE degradation (%)	Response 2 TOC removal (%)
			A: PHE concentration micrograms (l)	Factor 2 B: Catalyst dosage (g/l)	Factor 3 C: pH		
1	1	Block 1	1000.00	0.50	6.10	83.5	67.2
8	2	Block 1	1100.00	0.50	6.10	70.8	61.2
7	3	Block 1	1300.00	0.50	6.10	61	58.1
5	4	Block 1	1400.00	0.50	6.10	51.3	52.4
12	5	Block 1	1500.00	0.50	6.10	43	41.4
4	6	Block 1	1000.00	0.10	6.10	50.1	66.9
10	7	Block 1	1000.00	0.30	6.10	67.9	62.8
9	8	Block 1	1000.00	0.50	6.10	83.5	58.1
2	9	Block 1	1000.00	0.70	6.10	73.1	52.3
11	10	Block 1	1000.00	0.90	6.10	46.1	49.1
6	11	Block 1	1000.00	0.50	3.00	89.8	67.5
3	12	Block 1	1000.00	0.50	6.10	83.5	61.2
18	13	Block 2	1000.00	0.50	7.00	63.6	61.6
19	14	Block 2	1250.00	0.30	0.50	61.4	63.1
17	15	Block 2	1250.00	0.30	9.00	80.5	48.3
14	16	Block 2	1250.00	0.50	6.00	78.7	60.1
16	17	Block 2	1200.00	0.10	6.00	65.3	61.2
13	18	Block 2	1000.00	0.50	6.00	86.5	64.1
15	19	Block 2	1250.00	0.50	6.00	76.4	66.1
20	20	Block 2	1250.00	0.30	6.00	79.8	61.2

Table 4. ANOVA results of quadratic model for PHE degradation efficiency (Y_1)

PHE degradation efficiency					
ANOVA for response surface quadratic model					
Analysis of variance table (partial sum of squares – type III)					
Source	Sum of squares	df	Mean square	F value	P value Prob > F
Block	239.14	1	239.14		
Model	3336.58	9	370.73	14.14	0.0003 significant
A: PHE concentration	7.90	1	7.90	0.30	0.5965
B: Catalyst dosage	330.79	1	330.79	12.62	0.0062
C: pH	175.81	1	175.81	6.71	0.0292
AB	372.94	1	373.94	14.22	0.0044
AC	162.16	1	162.16	6.19	0.0346
BC	178.21	1	178.21	6.80	0.0284
A ²	1.93	1	1.93	0.074	0.7923
B ²	1471.16	1	1471.16	56.11	<0.0001
C ²	134.64	1	134.64	5.14	0.0497

Std. dev. 5.12; mean = 66.79; CV% = 7.34; R^2 = 0.9340; Adj. R^2 = 0.868; Adeq. precision = 12.976; Lack of fit = 6; Residuals = 9.

ANOVA quadratic model for PHE degradation and TOC removal efficiencies are illustrated in Tables 4 and 5. The large F -value of the model (14.14 and 9.89 for PHE degradation and TOC removal efficiencies) and 'Prob > F ' less than 0.5000 indicates that the terms of the model are

significant and there is only 0.11% chance that this could happen due to noise. In this case, the model terms B, C, AB, AC, BC, B², C² and A, A², C² are significant for the responses of PHE degradation and TOC removal respectively. Furthermore, the adequate precision value (12.976

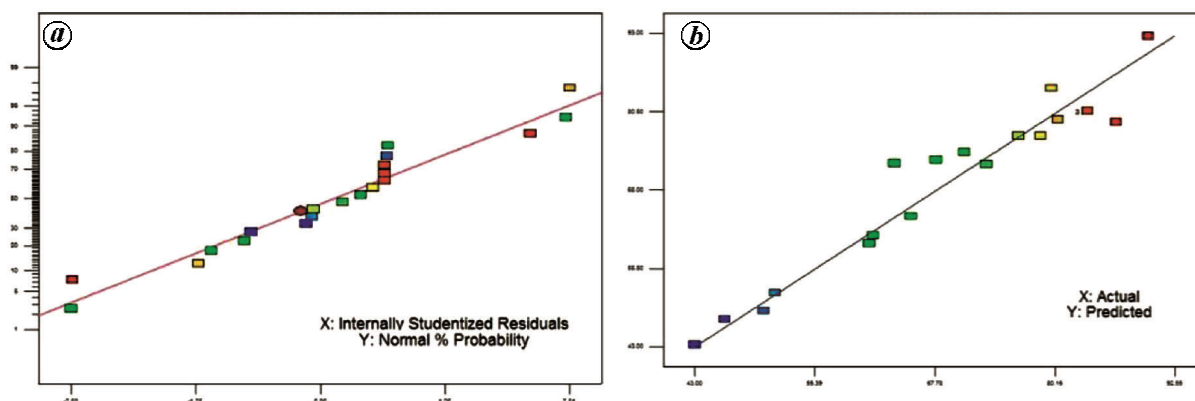


Figure 5. Photocatalytic degradation of PHE: (a) Normal probability plot of residuals and (b) predicted versus actual values.

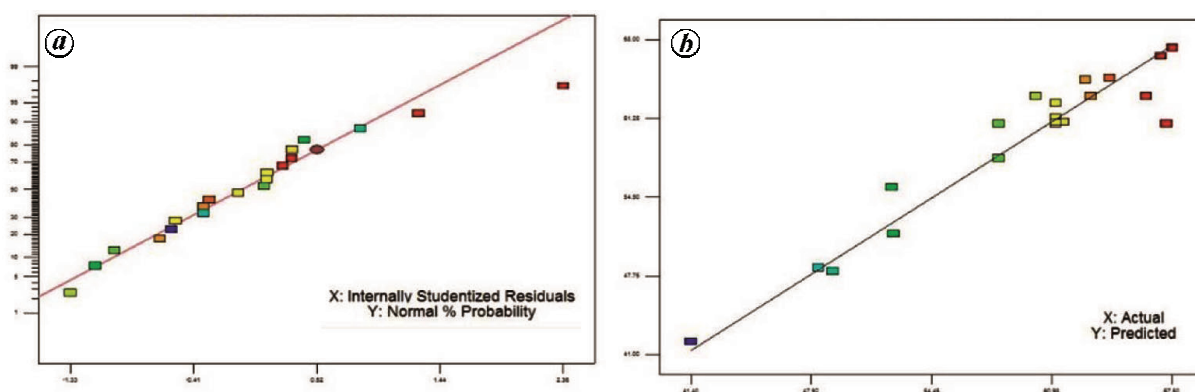


Figure 6. TOC removal: (a) Normal probability plot of residuals and (b) predicted versus actual values.

Table 5. ANOVA results of quadratic model for TOC removal efficiency (Y_1)

Response 2	TOC removal efficiency				
	ANOVA for response surface quadratic model				
	Analysis of variance table (partial sum of squares – type III)				
Source	Sum of squares	df	Mean square	F value	P value Prob > F
Block	30.70	1	30.70		
Model	833.52	9	92.61	9.89	0.0011 significant
A: PHE concentration	64.47	1	64.47	6.89	0.0276
B: Catalyst dosage	2.68	1	2.68	0.29	0.6057
C: pH	0.16	1	0.16	0.017	0.8987
AB	17.74	1	17.74	1.90	0.2019
AC	0.47	1	0.47	0.050	0.8280
BC	0.41	1	0.41	0.050	0.8280
A ²	72.63	1	72.63	7.76	0.0212
B ²	16.46	1	16.46	1.76	0.2175
C ²	53.17	1	53.17	5.68	0.0410

Std. dev. 3.06; Mean = 59.19; CV% = 5.17; $R^2 = 0.9082$; Adj. $R^2 = 0.815$; Adeq. precision = 11.094; Lack of fit = 6 and residuals = 9.

and 11.094) for PHE degradation and TOC removal efficiencies >4, also confirms that the model is adequate. Lack of fit test is a sign of lacking of experimental data for a model for which the model cannot calculate random errors. Lack of fit = 6 indicates a valid LOF test in which case minimum 3 is recommended. It can also be seen that there is a good correlation between the predicted values and experimental data and hence the data fitted well with

the range studied. This could be confirmed with the plot of predicted versus actual response (Figure 5) and the normal probability plot of residuals (Figure 6). The residuals falling on a straight line confirm the normal distribution of errors.

Figure 7 a–d are the three-dimensional response surface plots and the graphical representation of the regression eqs (2) and (3). At the initial stage, the increase in

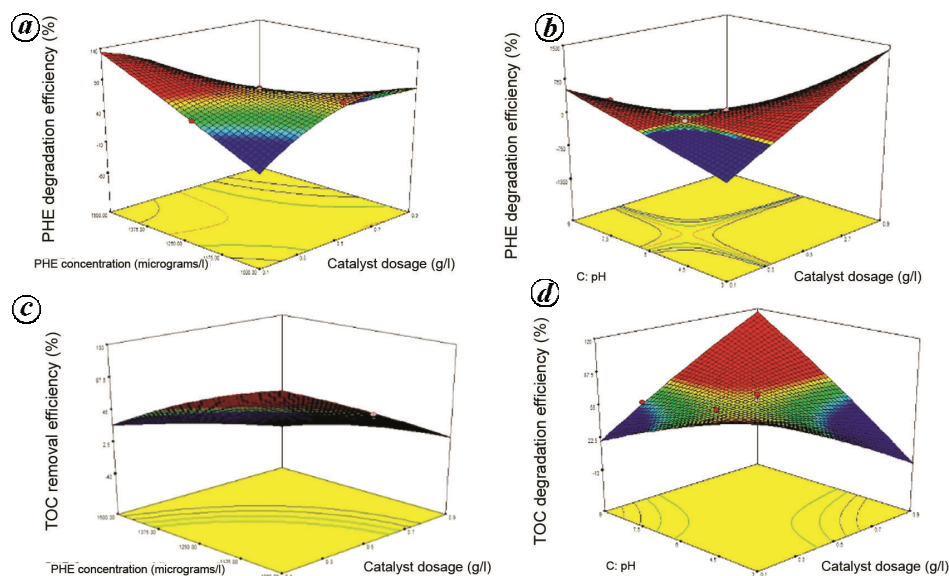


Figure 7. Response surface methodology 3D surface plots for PHE removal (a) and (b) and TOC removal (c) and (d).

TiO₂ photocatalyst dosage increased the PHE degradation efficiency due to the availability of sufficient active sites. However further increase in TiO₂ photocatalyst dosage decreased the degradation efficiency. This may be due to light screening and scattering effects, as well as the photocatalyst particle agglomeration^{26,41}. The degradation efficiency did not increase after 0.5 g/l (optimum value) of TiO₂. On the contrary, increase in PHE concentration, showed negative effect on degradation and TOC removal efficiency. This may be due to the inadequate availability of hydroxyl radicals as their amount needed is more at higher concentrations. Furthermore, at acidic pH, the higher PHE and TOC removal obtained may be due to the surface charge of TiO₂. Similar observations were made in various studies for different compounds such as dyes⁴² (acid blue 92 and basic blue 3) and triclosan⁴³.

Conclusion

A slurry photocatalytic reactor was evaluated for PHE removal. Batch studies were carried out and the maximum PHE degradation and TOC removal efficiencies obtained were 84% and 60% respectively for optimized conditions. The optimized parameters were: (PHE) = 1000 µg/l, (TiO₂) dosage = 0.5 g/l, pH = 3. During these experiments it was observed that the initial PHE concentration affected the degradation efficiency significantly and maximum degradation was obtained at lower initial concentration and at lower pH. The experimental data was well fitted to pseudo first-order kinetics and analysed with RSM modelling. Design expert software was used to analyse the obtained data. The experimental results obtained from continuous experiments indicated that the slurry reactor has a potential for long term operations.

1. Gevao, B., Jones, K. C. and Hamilton, T. J., Polycyclic aromatic hydrocarbon (PAH) deposition in a small rural lake Cumbria, UK. *Sci. Total Environ.*, 1998, **215**, 231–242.
2. Gao, Y. Z. and Zhu, L. Z., Plant uptake, accumulation and translocation of phenanthrene and pyrene in soil. *Chemosphere*, 2004, **127**(1), 131–139.
3. Baek, S., Goldstone, M., Kirk, P., Lester, J. and Perry, R., Phase distribution and particle size dependency of polycyclic aromatic hydrocarbons in the urban atmosphere. *Chemosphere*, 1991, **22**, 503–520.
4. NRC (National Research Council), Polycyclic aromatic hydrocarbons: Evaluation of sources and effects. National Academy Press ES/I-ES/7, Washington, DC, 1983.
5. Burn, G., Vaidya, O. and Leger, M., Atmospheric deposition of polycyclic aromatic hydrocarbons to Atlantic, Canada: geographic and temporal distributions and trends 1980–2001. *Environ. Sci. Technol.*, 2004, **38**, 1941–1948.
6. Clemons, J., Allan, C., Marvin, C., Wu, Z., McCarry, B. and Bryant, D., Evidence of estrogen and TCDD-like activities in crude and fractionated extracts of PM 10 air particulate material using *in vitro* gene expression assays. *Environ. Sci. Technol.*, 2004, **32**, 1853–1860.
7. Shi, Z. *et al.*, Contamination of rivers in Tianjin, China by polycyclic aromatic hydrocarbons. *Environ. Pollut.*, 2005, **134**, 97–111.
8. Kveseth, K., Sortland, B. and Bokn, T., Aromatic hydrocarbons in sewage mussels and tap water. *Chemosphere*, 1982, **11**, 623–639.
9. Vela, N., Martinez-Menchon, M., Navarro, G., Perez-Lucas, G. and Navarro, S., Removal of polycyclic aromatic hydrocarbons (PAHs) from ground water by heterogeneous photocatalysis under natural sunlight. *J. Photochem. Photobiol. A Chem.*, 2012, **232**, 32–40.
10. Comminellis, A., Kapalka, A., Malato, S., Parsons, S. A., Poullos, I. and Mantzavinos, D., Advanced oxidation processes for water treatment: advances and trends for R&D. *J. Chem. Technol. Biotechnol.*, 2008, **83**(1), 769–776.
11. Sanches, S., Crespo, M. T. B. and Pereira, V. J., Drinking water treatment of priority pesticides using low pressure UV photolysis and advanced oxidation processes. *Water Res.*, 2010, **44**(6), 1809–1818.

12. Sanches, S. *et al.*, Direct photolysis of polycyclic aromatic hydrocarbons in drinking water sources. *J. Hazard. Mater.*, 2011, **192**(3), 1458–1465.
13. Anandan, S., Vinu, A., Mori, T., Gokulakrishnan, N., Murugesan, V. and Ariga, K., Photocatalytic degradation of 2,4,6-trichlorophenol using lanthanum doped ZnO in aqueous suspension. *Catal. Commun.*, 2007, **8**(9), 1377–1382.
14. Bayarri, B., Gimenez, J., Curco, D. and Esplugas, S., Photocatalytic degradation of 2,4-dichlorophenol by TiO₂/UV: kinetics, actinometrics and models. *Catal. Today*, 2005, **101**(3-4), 227–236.
15. Huang, C. P., Dong, C. and Tang, Z., Advanced chemical oxidation: Its present role and potential future in hazardous waste treatment. *Waste Manage.*, 1993, **13**, 361–377.
16. Kormann, C., Bahnemann, D. W. and Hoffmann, M. R., Preparation and characterization of quantum-size titanium dioxide. *J. Phys. Chem.*, 1988, **92**(18), 5196–5201.
17. Bahnemann, D., Cunningham, J., Fox, M. A., Pelizzetti, E., Pichat, P. and Serpone, N., In *Aquatic and Surface Photochemistry* (eds Helz, G. R., Zepp, R. G. and Crosby), Lewis Publishers, Boca Raton, 1994, p. 261.
18. Theurich, J., Bahnemann, D., Vogel, R., Ehmed, F. E., Alhakimi, G. and Rajab, I., Photocatalytic degradation of naphthalene and anthracene: GC-MS analysis of the degradation pathway. *Res. Chem. Intermed.*, 1997, **23**(3), 247–274.
19. Woo, O. T., Chung, W. K., Wong, K. H. and Chow, A. T., Photocatalytic oxidation of polycyclic aromatic hydrocarbons: intermediates identification and toxicity testing. *J. Hazard. Mater.*, 2009, **168**(2–3), 1192–1199.
20. Gu, J., Dong, D., Kong, L., Zheng, Y. and Li, X., Photocatalytic degradation of phenanthrene on soil surfaces in the presence of nanometer anatase TiO₂ under UV-light. *J. Environ. Sci.*, 2012, **24**(12), 2122–2126.
21. Lin, H. F. and Valsaraj, K. T., A titania thin film annular photocatalytic reactor for the degradation of polycyclic aromatic hydrocarbons in dilute water streams. *J. Hazard. Mater.*, 2003, **99**, 203–219.
22. Vela, N., Mart'inez-Mench'on, G., Navarro, G., P'erez-Lucas and Navarro, S., Removal of polycyclic aromatic hydrocarbons (PAHs) from groundwater by heterogeneous photocatalysis under natural sunlight. *J. Photochem. Photobiol. A: Chem.*, 2012, **232**, 32–40.
23. Zhang, L., Li, P., Gong, Z. and Li, X., Photocatalytic degradation of polycyclic aromatic hydrocarbons on soil surfaces using TiO₂ under UV light. *J. Hazard. Mater.*, 2008, **158**, 478–484.
24. Liu, B., Chen, B., Zhang, B. Y. and Jing, L., Photocatalytic degradation of polycyclic aromatic hydrocarbons in offshore produced water: effects of water matrix. *J. Environ. Eng.*, 2016, **142**(11), 04016054 (1–7).
25. Asadi, M., Shayegan, J. and Alaie, E., Photocatalytic degradation of PAHs contaminated soil in south pars economical and energy zone with TiO₂ nanocatalyst. *Iran J. Chem. Eng.*, 2007, **4**(1), 14–20.
26. Callahan, M. A. *et al.*, Water related environmental fate of 129 priority pollutants. US Environmental Protection Agency, Washington DC, 1979, EPA-440/4-79-029.
27. Konstantinou, I. K. and Albanis, T. A., TiO₂ assisted photocatalytic degradation of azo dyes in aqueous solution: kinetic and mechanistic investigations: A review. *Appl. Catal. B: Environ.*, 2004, **49**(1), 1–14.
28. Mills, A., Davis, R. H. and Worsley, D., Water purification by semiconductor photocatalysis. *Chem. Soc. Rev.*, 1993, **22**, 417–487.
29. Poullos, I. and Aetopoulou, I., Photocatalytic degradation of the textile dye Reactive Orange 16 in the presence of TiO₂ suspensions. *Environ. Sci. Technol.*, 1999, **20**(5), 479–487.
30. So, C. M., Cheng, M. Y., Yu, J. C. and Wong, P. K., Degradation of azo dye Procion Red MX-5B by photocatalytic oxidation. *Chemosphere*, 2002, **46**, 905–912.
31. Damodar, R. A., You, S.-J. and Qu, S.-H., Coupling of membrane separation with photocatalytic slurry reactor for advanced dye wastewater treatment. *Sep. Purif. Technol.*, 2010, **76**, 64–71.
32. Neppolian, B., Choi, H. C., Sakthivel, S., Arabindoo, B. and Murugesan, V., Solar/UV-induced photocatalytic degradation of three commercial textile dyes. *J. Hazard. Mater.*, 2002, **89**(2–3), 303–317.
33. Muruganandham, M. and Swaminathan, M., Photocatalytic decolorization and degradation of orange 4 by TiO₂-UV process. *Dyes. Pigm.*, 2006, **68**, 133–142.
34. Laohaprapanon, A., Matahumb, J., Tayob, L. and Youa, S., Photodegradation of reactive black 5 in a ZnO/UV slurry membrane reactor. *J. Taiwan Inst. Chem. Eng.*, 2015, **49**, 136–141.
35. Fernandez, R. L., McDonald, J. A., Khan, S. J. and Clech, P. L., Removal of pharmaceuticals and endocrine disrupting chemicals by a submerged membrane photocatalysis reactor (MPR). *Sep. Purif. Technol.*, 2014, **127**(1), 131–139.
36. Mozia, S., Photocatalytic membrane reactors (PMR) in water and wastewater treatment. *Sep. Purif. Technol.*, 2010, **73**(2), 71–91.
37. Davis, R. J., Gainer, J. L., Neal, G. O. and Wenwu, I., Photocatalytic decolorization of wastewater dyes. *Water Environ. Res.*, 1994, **66**, 50–53.
38. Zhang, L., Liu, C. Y. and Ren, X. M., Photochemistry of semiconductor particles. Part 4 – Effects of surface condition on the photodegradation of 2,4-dichlorophenol catalyzed by TiO₂ suspensions. *J. Photochem. Photobiol. A Chem.*, 1995, **85**, 239–245.
39. Sakthivel, S., Neppolian, B., Shankar, M. V., Palanichamy, M. and Murugesan, V., Solar photocatalytic degradation of azo dye: comparison of photocatalytic efficiency of ZnO and TiO₂. *Sol. Energy Mater. Sol. Cells*, 2003, **77**(1), 65–82.
40. Nashio, J., Tokumura, M., Znad, H. T. and Kawase, Y., Photocatalytic decolorization of azo dye with zinc oxide powder in an external UV light irradiation slurry photoreactor. *J. Hazard. Mater.*, 2006, **138**, 106–115.
41. Antonopoulou, M., Papadopoulos, V. and Konstantinou, I., Photocatalytic oxidation of treated municipal wastewaters for the removal of phenolic compounds: optimization and modeling using response surface methodology (RSM) and artificial neural networks (ANNs). *J. Chem. Technol. Biotechnol.*, 2012, **87**(10), 1385–1395.
42. Fathinia, M., Khataee, A. R., Zarei, M. and Aber, S., Comparative photocatalytic degradation of two dyes on immobilized TiO₂ nanoparticles: effect of dye molecular structure and response surface approach. *J. Mol. Catal. A Chem.*, 2010, **333**(1-2), 73–84.
43. Stamatis, N., Antonopoulou, M., Hela, D. and Konstantinou, I., Photocatalytic degradation kinetics and mechanisms of antibacterial triclosan in aqueous TiO₂ suspensions under simulated solar irradiation. *J. Chem. Technol. Biotechnol.*, 2014, **89**(8), 1145–1154.

ACKNOWLEDGEMENTS. We acknowledge the University Grants Commission (UGC), New Delhi for financial support while carrying out this study. We also acknowledge Murugappa Chettiar Research Centre (MCRC), Taramani for granting access to TOC analysis.

Received 19 February 2018; accepted 21 May 2018

doi: 10.18520/cs/v115/i9/1732-1740